

Production of e^+e^- pairs accompanied by nuclear dissociation in ultraperipheral heavy-ion collisions

J. Adams,² M. M. Aggarwal,²⁸ Z. Ahammed,⁴² J. Amonett,¹⁹ B. D. Anderson,¹⁹ D. Arkhipkin,¹² G. S. Averichev,¹¹ Y. Bai,²⁶ J. Balewski,¹⁶ O. Barannikova,³¹ L. S. Barnby,² J. Baudot,¹⁷ S. Bekele,²⁷ V. V. Belaga,¹¹ R. Bellwied,⁴⁵ J. Berger,¹³ B. I. Bezverkhny,⁴⁷ S. Bharadwaj,³² V. S. Bhatia,²⁸ H. Bichsel,⁴⁴ A. Billmeier,⁴⁵ L. C. Bland,³ C. O. Blyth,² B. E. Bonner,³³ M. Botje,²⁶ A. Boucham,³⁷ A. Brandin,²⁴ A. Bravar,³ M. Bystersky,¹⁰ R. V. Cadman,¹ X. Z. Cai,³⁶ H. Caines,⁴⁷ M. Calderón de la Barca Sánchez,³ J. Carroll,²⁰ J. Castillo,²⁰ D. Ceбра,⁶ Z. Chajecski,⁴³ P. Chaloupka,¹⁰ S. Chattopdhyay,⁴² H. F. Chen,³⁵ Y. Chen,⁷ J. Cheng,⁴⁰ M. Cherney,⁹ A. Chikhanian,⁴⁷ W. Christie,³ J. P. Coffin,¹⁷ T. M. Cormier,⁴⁵ J. G. Cramer,⁴⁴ H. J. Crawford,⁵ D. Das,⁴² S. Das,⁴² M. M. de Moura,³⁴ A. A. Derevschikov,³⁰ L. Didenko,³ T. Dietel,¹³ W. J. Dong,⁷ X. Dong,³⁵ J. E. Draper,⁶ F. Du,⁴⁷ A. K. Dubey,¹⁴ V. B. Dunin,¹¹ J. C. Dunlop,³ M. R. Dutta Mazumdar,⁴² V. Eckardt,²² W. R. Edwards,²⁰ L. G. Efimov,¹¹ V. Emelianov,²⁴ J. Engelage,⁵ G. Eppley,³³ B. Erasmus,³⁷ M. Estienne,³⁷ P. Fachini,³ J. Faivre,¹⁷ R. Fatemi,¹⁶ J. Fedorisin,¹¹ K. Filimonov,²⁰ P. Filip,¹⁰ E. Finch,⁴⁷ V. Fine,³ Y. Fisyak,³ K. J. Foley,³ K. Fomenko,¹¹ J. Fu,⁴⁰ C. A. Gagliardi,³⁸ J. Gans,⁴⁷ M. S. Ganti,⁴² L. Gaudichet,³⁷ F. Geurts,³³ V. Ghazikhanian,⁷ P. Ghosh,⁴² J. E. Gonzalez,⁷ O. Grachov,⁴⁵ O. Grebenyuk,²⁶ D. Grosnick,⁴¹ S. M. Guertin,⁷ Y. Guo,⁴⁵ A. Gupta,¹⁸ T. D. Gutierrez,⁷ J. J. Hallman,³ A. Hamed,⁴⁵ D. Hardtke,²⁰ J. W. Harris,⁴⁷ M. Heinz,⁴⁷ T. W. Henry,³⁸ S. Heppelmann,²⁹ B. Hippolyte,⁴⁷ A. Hirsch,³¹ E. Hjort,²⁰ G. W. Hoffmann,³⁹ H. Z. Huang,⁷ S. L. Huang,³⁵ E. W. Hughes,⁴ T. J. Humanic,²⁷ G. Igo,⁷ A. Ishihara,³⁹ P. Jacobs,²⁰ W. W. Jacobs,¹⁶ M. Janik,⁴³ H. Jiang,⁷ P. G. Jones,² E. G. Judd,⁵ S. Kabana,⁴⁷ K. Kang,⁴⁰ M. Kaplan,⁸ D. Keane,¹⁹ V. Yu. Khodyrev,³⁰ J. Kiryluk,²¹ A. Kisiel,⁴³ E. M. Kislov,¹¹ J. Klay,²⁰ S. R. Klein,²⁰ A. Klyachko,¹⁶ D. D. Koetke,⁴¹ T. Kollegger,¹³ M. Kopytine,¹⁹ L. Kotchenda,²⁴ M. Kramer,²⁵ P. Kravtsov,²⁴ V. I. Kravtsov,³⁰ K. Krueger,¹ C. Kuhn,¹⁷ A. I. Kulikov,¹¹ A. Kumar,²⁸ C. L. Kunz,⁸ R. Kh. Kutuev,¹² A. A. Kuznetsov,¹¹ M. A.C. Lamont,² J. M. Landgraf,³ S. Lange,¹³ F. Laue,³ J. Lauret,³ A. Lebedev,³ R. Lednicky,¹¹ S. Lehocka,¹¹ M. J. LeVine,³ C. Li,³⁵ Q. Li,⁴⁵ Y. Li,⁴⁰ S. J. Lindenbaum,²⁵ M. A. Lisa,²⁷ F. Liu,⁴⁶ L. Liu,⁴⁶ Q. J. Liu,⁴⁴ Z. Liu,⁴⁶ T. Ljubicic,³ W. J. Llope,³³ H. Long,⁷ R. S. Longacre,³ M. Lopez-Noriega,²⁷ W. A. Love,³ Y. Lu,⁴⁶ T. Ludlam,³ D. Lynn,³ G. L. Ma,³⁶ J. G. Ma,⁷ Y. G. Ma,³⁶ D. Magestro,²⁷ S. Mahajan,¹⁸ D. P. Mahapatra,¹⁴ R. Majka,⁴⁷ L. K. Mangotra,¹⁸ R. Manweiler,⁴¹ S. Margetis,¹⁹ C. Markert,⁴⁷ L. Martin,³⁷ J. N. Marx,²⁰ H. S. Matis,²⁰ Yu. A. Matulenko,³⁰ C. J. McClain,¹ T. S. McShane,⁹ F. Meissner,²⁰ Yu. Melnick,³⁰ A. Meschanin,³⁰ M. L. Miller,²¹ Z. Milosevich,⁸ N. G. Minaev,³⁰ C. Mironov,¹⁹ A. Mischke,²⁶ D. Mishra,¹⁴ J. Mitchell,³³ B. Mohanty,⁴² L. Molnar,³¹ C. F. Moore,³⁹ M. J. Mora-Corral,²² D. A. Morozov,³⁰ V. Morozov,²⁰ M. G. Munhoz,²⁴ B. K. Nandi,⁴² T. K. Nayak,⁴² J. M. Nelson,² P. K. Netrakanti,⁴² V. A. Nikitin,¹² L. V. Nogach,³⁰ B. Norman,¹⁹ S. B. Nurushev,³⁰ G. Odyniec,²⁰ A. Ogawa,³ V. Okorokov,²⁴ M. Oldenburg,²⁰ D. Olson,²⁰ S. K. Pal,⁴² Y. Panebratsev,¹¹ S. Y. Panitkin,³ A. I. Pavlinov,⁴⁵ T. Pawlak,⁴³ T. Peitzmann,²⁶ V. Perevoztchikov,³ C. Perkins,⁵ W. Peryt,⁴³ V. A. Petrov,¹² S. C. Phatak,¹⁴ R. Picha,⁶ M. Planinic,⁴⁸ J. Pluta,⁴³ N. Porile,³¹ J. Porter,³ A. M. Poskanzer,²⁰ M. Potekhin,³ E. Potrebenikova,¹¹ B. V.K.S. Potukuchi,¹⁸ D. Prindle,⁴⁴ C. Pruneau,⁴⁵ J. Putschke,²² G. Rai,²⁰ G. Rakness,²⁹ R. Raniwala,³² S. Raniwala,³² O. Ravel,³⁷ R. L. Ray,³⁹ S. V. Razin,¹¹ D. Reichhold,³¹ J. G. Reid,⁴⁴ G. Renault,³⁷ F. Retiere,²⁰ A. Ridiger,²⁴ H. G. Ritter,²⁰ J. B. Roberts,³³ O. V. Rogachevskiy,¹¹ J. L. Romero,⁶ A. Rose,⁴⁵ C. Roy,³⁷ L. Ruan,³⁵ I. Sakrejda,²⁰ S. Salur,⁴⁷ J. Sandweiss,⁴⁷ I. Savin,¹² P. S. Sazhin,¹¹ J. Schambach,³⁹ R. P. Scharenberg,³¹ N. Schmitz,²² L. S. Schroeder,²⁰ K. Schweda,²⁰ J. Seger,⁹ P. Seyboth,²² E. Shahaliev,¹¹ M. Shao,³⁵ W. Shao,⁴ M. Sharma,²⁸ W. Q. Shen,³⁶ K. E. Shestermanov,³⁰ S. S. Shimanskiy,¹¹ F. Simon,²² R. N. Singaraju,⁴² G. Skoro,¹¹ N. Smirnov,⁴⁷ R. Snellings,²⁶ G. Sood,⁴¹ P. Sorensen,²⁰ J. Sowinski,¹⁶ J. Speltz,¹⁷ H. M. Spinka,¹ B. Srivastava,³¹ A. Stadnik,¹¹ T. D.S. Stanislaus,⁴¹ R. Stock,¹³ A. Stolpovsky,⁴⁵ M. Strikhanov,²⁴ B. Stringfellow,³¹ A. A.P. Suaide,³⁴ E. Sugarbaker,²⁷ C. Suire,³ M. Sumera,¹⁰ B. Surrow,²¹ T. J.M. Symons,²⁰ A. Szanto de Toledo,³⁴ P. Szarwas,⁴³ A. Tai,⁷ J. Takahashi,³⁴ A. H. Tang,²⁶ T. Tarnowsky,³¹ D. Thein,⁷ J. H. Thomas,²⁰ S. Timoshenko,²⁴ M. Tokarev,¹¹ T. A. Trainor,⁴⁴ S. Trentalange,⁷ R. E. Tribble,³⁸ O. Tsai,⁷ J. Ulery,³¹ T. Ullrich,³ D. G. Underwood,¹ A. Urkinbaev,¹¹ G. Van Buren,³ M. van Leeuwen,²⁰ A. M. Vander Molen,²³ R. Varma,¹⁵ I. M. Vasilevski,¹² A. N. Vasiliev,³⁰ R. Vernet,¹⁷ S. E. Vigdor,¹⁶ V. P. Viyogi,⁴² S. Vokal,¹¹ S. A. Voloshin,⁴⁵ M. Vznuzdaev,²⁴ B. Waggoner,⁹ F. Wang,³¹ G. Wang,¹⁹ G. Wang,⁴ X. L. Wang,³⁵ Y. Wang,³⁹ Y. Wang,⁴⁰ Z. M. Wang,³⁵ H. Ward,³⁹ J. W. Watson,¹⁹ J. C. Webb,¹⁶ R. Wells,²⁷ G. D. Westfall,²³ A. Wetzler,²⁰ C. Whitten, Jr.,⁷ H. Wieman,²⁰ S. W. Wissink,¹⁶ R. Witt,⁴⁷ J. Wood,⁷ J. Wu,³⁵ N. Xu,²⁰ Z. Xu,³⁵ Z. Z. Xu,³ E. Yamamoto,²⁰ P. Yepes,³³ V. I. Yurevich,¹¹ Y. V. Zanevsky,¹¹ H. Zhang,³ W. M. Zhang,¹⁹ Z. P. Zhang,³⁵ P. A. Zolnierczuk,¹⁶ R. Zoukharneev,¹² Y. Zoukharneeva,¹² and A. N. Zubarev¹¹

(STAR Collaboration*)

¹Argonne National Laboratory, Argonne, Illinois 60439, USA

²University of Birmingham, Birmingham, United Kingdom

³Brookhaven National Laboratory, Upton, New York 11973, USA

⁴California Institute of Technology, Pasadena, California 91125, USA

⁵University of California, Berkeley, California 94720, USA

⁶University of California, Davis, California 95616, USA

⁷University of California, Los Angeles, California 90095, USA

⁸Carnegie Mellon University, Pittsburgh, Pennsylvania 15213, USA

- ⁹Creighton University, Omaha, Nebraska 68178, USA
¹⁰Nuclear Physics Institute AS CR, 250 68 Řež/Prague, Czech Republic
¹¹Laboratory for High Energy (JINR), Dubna, Russia
¹²Particle Physics Laboratory (JINR), Dubna, Russia
¹³University of Frankfurt, Frankfurt, Germany
¹⁴Institute of Physics, Bhubaneswar 751005, India
¹⁵Indian Institute of Technology, Mumbai, India
¹⁶Indiana University, Bloomington, Indiana 47408, USA
¹⁷Institut de Recherches Subatomiques, Strasbourg, France
¹⁸University of Jammu, Jammu 180001, India
¹⁹Kent State University, Kent, Ohio 44242, USA
²⁰Lawrence Berkeley National Laboratory, Berkeley, California 94720, USA
²¹Massachusetts Institute of Technology, Cambridge, Massachusetts 02139-4307, USA
²²Max-Planck-Institut für Physik, Munich, Germany
²³Michigan State University, East Lansing, Michigan 48824, USA
²⁴Moscow Engineering Physics Institute, Moscow, Russia
²⁵City College of New York, New York City, New York 10031, USA
²⁶NIKHEF, Amsterdam, The Netherlands
²⁷Ohio State University, Columbus, Ohio 43210, USA
²⁸Panjab University, Chandigarh 160014, India
²⁹Pennsylvania State University, University Park, Pennsylvania 16802, USA
³⁰Institute of High Energy Physics, Protvino, Russia
³¹Purdue University, West Lafayette, Indiana 47907, USA
³²University of Rajasthan, Jaipur 302004, India
³³Rice University, Houston, Texas 77251, USA
³⁴Universidade de Sao Paulo, Sao Paulo, Brazil
³⁵University of Science & Technology of China, Anhui 230027, China
³⁶Shanghai Institute of Applied Physics, Shanghai 201800, People's Republic of China
³⁷SUBATECH, Nantes, France
³⁸Texas A & M University, College Station, Texas 77843, USA
³⁹University of Texas, Austin, Texas 78712, USA
⁴⁰Tsinghua University, Beijing, People's Republic of China
⁴¹Valparaiso University, Valparaiso, Indiana 46383, USA
⁴²Variable Energy Cyclotron Centre, Kolkata 700064, India
⁴³Warsaw University of Technology, Warsaw, Poland
⁴⁴University of Washington, Seattle, Washington 98195, USA
⁴⁵Wayne State University, Detroit, Michigan 48201, USA
⁴⁶Institute of Particle Physics, CCNU (HZNU), Wuhan 430079, China
⁴⁷Yale University, New Haven, Connecticut 06520, USA
⁴⁸University of Zagreb, Zagreb, HR-10002, Croatia
- (Received 7 April 2004; published 28 September 2004)

We present data on e^+e^- pair production accompanied by nuclear breakup in ultraperipheral gold-gold collisions at a center of mass energy of 200 GeV per nucleon pair. The nuclear breakup requirement selects events at small impact parameters, where higher-order diagrams for pair production should be enhanced. We compare the data with two calculations: one based on the equivalent photon approximation, and the other using lowest-order quantum electrodynamics (QED). The data distributions agree with both calculations, except that the pair transverse momentum spectrum disagrees with the equivalent photon approach. We set limits on higher-order contributions to the cross section.

DOI: 10.1103/PhysRevC.70.031902

PACS number(s): 25.75.Dw, 12.20.-m, 25.20.Lj

Electron-positron pairs are copiously produced by photon interactions in the strong electromagnetic fields of fully stripped colliding heavy nuclei (cf. Fig. 1); the field strength

at the surface of the ions reaches 10^{20} V/cm. At a center of mass energy of $\sqrt{s_{NN}}=200$ GeV per nucleon pair, the production cross section is expected to be 33000 b, or 4400 times the hadronic cross section [1,2].

*URL: <http://www.star.bnl.gov>

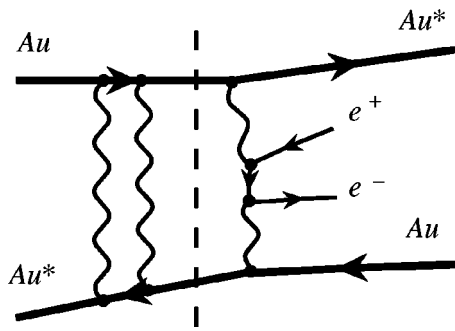


FIG. 1. Schematic QED lowest-order diagram for e^+e^- production accompanied by mutual Coulomb excitation. The dashed line shows the factorization into mutual Coulomb excitation and e^+e^- production.

The electromagnetic fields are strong enough, with coupling $Z\alpha \approx 0.6$ (Z is the nuclear charge and $\alpha \approx 1/137$ the fine-structure constant), that conventional perturbative calculations of the process are questionable. Many groups have studied higher-order calculations of pair production. Some early coupled-channel calculations predicted huge (order-of-magnitude) enhancements in the cross section [3] compared to lowest-order perturbative calculations.

Ivanov, Schiller, and Serbo [4] followed the Bethe-Maximon approach [5], and found that at the Relativistic Heavy Ion Collider (RHIC), Coulomb corrections to account for pair production in the electromagnetic potential of the ions reduce the cross section 25% below the lowest-order result. For high-energy real photons incident on a heavy atom, these Coulomb corrections are independent of the photon energy and depend only weakly on the pair-mass [5]. However, for intermediate-energy photons, there is a pair-mass dependence, and also a difference between the e^+ and e^- spectra due to interference between different order terms [6].

In contrast, initial all-orders calculations based on solving the Dirac equation exactly in the ultrarelativistic limit [7] found results that match the lowest-order perturbative result [8]. However, improved all-orders calculations have agreed with the Coulomb corrected calculation [9]. These all-orders calculations do not predict the kinematic distributions of the produced pairs.

Any higher-order corrections should be the largest close to the nuclei, where the photon densities are largest. These high-density regions have the largest overlap at small ion-ion impact parameters b . Small- b collisions can be selected by choosing events where the nuclei undergo Coulomb excitation, followed by dissociation. The dissociation also provides a convenient experimental trigger. Pair production accompanied by mutual Coulomb excitation should occur at smaller b , and have larger higher-order corrections than for unaccompanied pairs.

Previous measurements of e^+e^- pair production were at much lower energies [10,11]. The cross sections, pair-masses, angular and p_T distributions generally agreed with the leading-order QED perturbative calculations. These studies did not require that the nuclei break up, and so covered a wide range of impact parameters.

This letter reports on electromagnetic production of e^+e^- pairs accompanied by Coulomb nuclear breakup in $\sqrt{s_{NN}} = 200$ GeV per nucleon pair Au-Au collisions [12], as is shown in Fig. 1. An e^+e^- pair is produced from two photons, while the nuclei exchange additional, independent photons, which break up the nuclei. We require that there be no hadronic interactions, which is roughly equivalent to setting the minimum impact parameter b_{\min} at twice the nuclear radius, R_A , i.e., about 13 fm. The Coulomb nuclear breakup requirement selects moderate impact parameter collisions ($2R_A < b < \approx 30$ fm) [13,14]. Except for the common impact parameter, the mutual Coulomb dissociation is independent of the e^+e^- production [15,16]. The cross section is

$$\sigma(\text{AuAu} \rightarrow \text{Au}^* \text{Au}^* e^+ e^-) = \int d^2b P_{ee}(b) P_{2EXC}(b), \quad (1)$$

where $P_{ee}(b)$ and $P_{2EXC}(b)$ are the probabilities of e^+e^- production and mutual excitation, respectively, at impact parameter b . The decay of the excited nucleus usually involves neutron emission. $P_{2EXC}(b)$ is based on experimental studies of neutron emission in photodissociation [17]. For small b , a leading-order calculation of $P_{2EXC}(b)$ may exceed 1. A unitarization procedure is used to correct $P_{2EXC}(b)$ to account for multiple interactions [14,17].

The most common excitation is a giant dipole resonance (GDR). GDRs usually decay by single neutron emission. Other resonances decay to final states with higher neutron multiplicities. In mutual Coulomb dissociation, each nucleus emits a photon which dissociates the other nucleus. The neutrons are a distinctive signature for nuclear breakup.

We consider two different pair production calculations for $P_{ee}(b)$. The first uses the equivalent photon approach (EPA) [1], which is commonly used to study photoproduction. The photon flux from each nucleus is calculated using the Weizsäcker-Williams method. The photons are treated as if they were real [2]. The e^+e^- pair production is then calculated using the lowest-order diagram [18]. The photon p_T spectrum for a photon with energy k is given by [19,20]

$$\frac{dN}{dp_T} \approx \frac{F^2(k^2/\gamma^2 + p_T^2) p_T^2}{\pi^2 (k^2/\gamma^2 + p_T^2)^2}, \quad (2)$$

where F is the nuclear form factor and γ is the Lorentz boost of a nucleus in the laboratory frame. This calculation uses a Woods-Saxon distribution with a gold radius of 6.38 fm and a 0.535 fm skin thickness [21]. The individual photon p_T are added in quadrature to give the pair p_T . This is a minor simplification, but should have little effect on the result. For e^+e^- pairs visible in STAR, the typical photon $p_T \approx 3$ MeV/ c , for a pair $p_T \approx 5$ MeV/ c .

The second calculation is a lowest-order quantum electrodynamics (QED) calculation for pair production [22]. The main difference between this calculation and the EPA approach is that the QED calculation includes photon virtuality. In the relevant kinematic range, the results of the calculations differ mainly in the pair p_T spectrum [23]. In the QED calculation, the pair p_T is peaked at 20 MeV/ c , higher than with the EPA.

One unavoidable difficulty in studying this reaction at an ion collider is that e^+e^- pairs are dominantly produced with a forward-backward topology. The angle between the electron momentum and the two-photon axis in the two-photon rest frame, θ^* , is usually small. Only a small fraction of the pairs are visible in a central detector, limiting the statistics.

This analysis presents data taken in 2001 with the Solenoidal Tracker at the RHIC (STAR) detector at the Relativistic Heavy Ion Collider (RHIC). Tracks were reconstructed in a large cylindrical time projection chamber (TPC) [24] embedded in a solenoidal magnetic field. The track position and specific energy loss (dE/dx) were measured at 45 points at radii between 60 and 189 cm from the collision point. Many of the tracks used in this analysis had low transverse momenta p_T and curved strongly in the magnetic field, and therefore had less than 45 reconstructable points. This analysis used data taken in a 0.25 T magnetic field (half the usual value).

This analysis used about 800 000 events selected by a minimum bias trigger [25]. This trigger selected events where both gold nuclei broke up, by detecting events with one or more neutrons in zero degree calorimeters (ZDCs) [26] upstream and downstream of the collision point. The two ZDC hits were required to be within 1 nsec of each other. With the beam conditions and ZDC resolution, this selected events along the beam line within ≈ 30 cm of the detector center.

The signature for e^+e^- production is two reconstructed tracks which formed a primary vertex along the beamline and which had specific energy losses consistent with those of electrons. Event vertices were found by an iterative procedure [12]. The analysis accepted events with a vertex containing exactly two tracks. Up to two additional nonvertex tracks were allowed in the event, to account for random backgrounds.

Tracks were required to have $p_T > 65$ MeV/c and pseudorapidity $|\eta| < 1.15$. In this region, the tracking efficiency was above 80%. Tracks were also required to have momenta $p < 130$ MeV/c, where dE/dx allowed good electron/hadron separation. In this region, the identification efficiency was almost 100%, with minimal contamination. Pairs were required to have masses $140 \text{ MeV} < M_{ee} < 265$ MeV. The pair-mass spectrum falls steeply with increasing M_{ee} , so few leptons from pairs were expected with higher momenta. Pairs were required to have $p_T < 100$ MeV/c and rapidity $|Y| < 1.15$. The pair cuts remove a very few background events, but leave the signal intact. These cuts selected a sample of 52 events.

The data were corrected for efficiency using simulated events based on the equivalent photon calculation and the standard STAR detector simulation and reconstruction programs. The distributions of the number of hits and track fit quality, the vertex radial positions, and the track distance of closest approach matched in the data and simulations [12].

The resolutions were found to be 0.017 for pair rapidity, 0.01 for track rapidity, and 6 MeV for pair-mass. The pair p_T resolution varied slightly with p_T , but averaged about 4 MeV/c. After accounting for this p_T smearing, the efficiency was found to be independent of p_T .

There are two backgrounds in this analysis. Incoherent (mostly hadronic) backgrounds produce both like-sign and

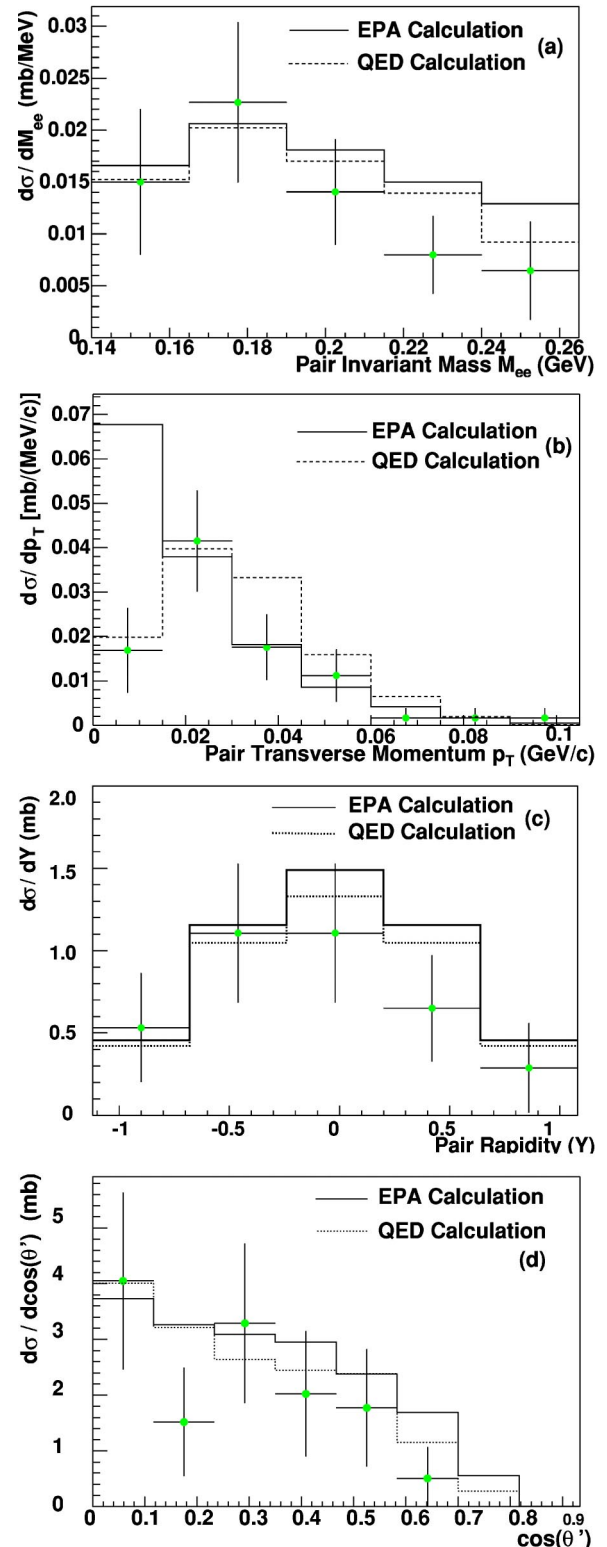


FIG. 2. (Color online) (a) The pair-mass distribution, (b) pair p_T , (c) pair rapidity, and (d) pair $\cos(\theta')$ distributions. The data (points) are compared with predictions from the EPA (solid histogram) and lowest-order QED (dashed histogram) calculations. The error bars include both statistical and systematic errors.

unlike-sign pairs, at a wide range of p_T . Based on a study of like-sign and of higher p_T pairs, we estimate that this background is 1 event. Coherent backgrounds are due to photo-production of misidentified $\pi^+\pi^-$ pairs on one of the nuclei. This background is peaked at higher M_{ee} than real e^+e^- pairs. From the known ρ^0 and direct $\pi^+\pi^-$ cross sections [13,21], and electron misidentification probabilities, the contamination is estimated to be less than 0.1 events. Backgrounds from other electromagnetic processes should be even smaller. The background from cosmic rays is suppressed to a negligible level by the ZDC coincidence requirement.

The luminosity was determined by counting hadronic interactions with at least eight charged tracks. This criteria selects 80% of all hadronic gold-gold interactions [12,27]. After compensating for the different neutron multiplicities in the hadronic and e^+e^- samples (the ZDC timing resolution depends on the number of neutrons) and assuming a total hadronic cross section of 7.2 barns [13], we find a total integrated luminosity of $94 \pm 9 \text{ mb}^{-1}$.

The major systematic errors were due to uncertainties in the tracking efficiency (6.4% per track, or 13% total), vertexing (8.5%), and in the luminosity (10%) [12]. The uncertainties due to backgrounds and particle identification were much smaller and are neglected. These uncertainties were added in quadrature, giving a 18.5% total systematic uncertainty.

Figure 2(a) shows the cross section for $\text{Au Au} \rightarrow \text{Au}^* \text{Au}^* e^+e^-$ as a function of pair-mass, within our kinematic fiducial region: track $p_T > 65 \text{ MeV}/c$, track pseudorapidity $|\eta| < 1.15$, pair rapidity $|Y| < 1.15$, and pair-mass $140 \text{ MeV} < M_{ee} < 265 \text{ MeV}$. The data are compared to the equivalent photon (solid) and QED (dashed) calculations. Monte Carlo events were generated using the two calculations, and then filtered to match the acceptances used here. Both calculations match the pair-mass data.

Figure 2(b) shows the cross section as a function of pair p_T . The equivalent photon (solid) and QED (dashed) calculations differ when $p_T < 15 \text{ MeV}/c$, due to the nonzero photon virtuality in the QED calculation. The data agree with the QED calculation, but not with the equivalent photon calculation.

Figure 2(c) shows the cross section as a function of pair rapidity. The broad peak around $Y=0$ is due to the detector acceptance. Selecting tracks with pseudorapidities $|\eta| < 1.15$ preferentially chooses events with small pair rapidity. The data agrees with both calculations.

Figure 2(d) shows the angular distribution $\cos(\theta')$ between the e^+ momentum and the beam axis in the pair rest frame. There is a small (usually $< 5 \text{ mrad}$) difference between θ' and θ^* since the photon p_T rotates the $\gamma\gamma$ rest frame slightly with respect to the beam axis. The distribution in Fig. 2(d) is the convolution of the detector acceptance [largest at small $\cos(\theta')$] with the production distribution, which is peaked at large $\cos(\theta')$. The agreement between the data and the calculations is good.

Within the kinematic range $140 \text{ MeV} < M_{ee} < 265 \text{ MeV}$, pair rapidity $|Y| < 1.15$, track $p_T > 65 \text{ MeV}/c$, and $|\eta| < 1.15$, the cross section $\sigma = 1.6 \pm 0.2(\text{stat}) \pm 0.3(\text{syst}) \text{ mb}$, in reasonable agreement with the equivalent photon prediction of 2.1 mb and the QED calculation of $\sigma_{\text{QED}} = 1.9 \text{ mb}$. At a 90%

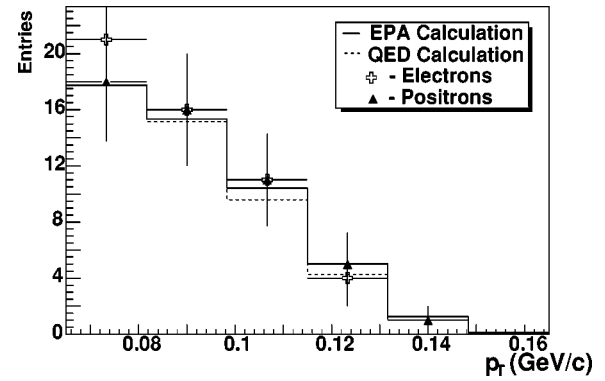


FIG. 3. The p_T spectra of the produced electrons and positrons, along with the comparable EPA and QED calculations. In both calculations, the electron and positron spectra are identical. Spectra from the two calculations are similar; the data agree with both of them.

confidence level, higher-order corrections to the cross section, $\Delta\sigma = \sigma - \sigma_{\text{QED}}$, must be within the range $-0.5\sigma_{\text{QED}} < \Delta\sigma < 0.2\sigma_{\text{QED}}$.

At leading order, the electron and positron momentum spectra are identical. However, interference with higher-order corrections can create charge-dependent spectral differences [6]. For some kinematic variables, 30–60% asymmetries may occur [28]. A study of e^+e^- production in sulfur-nucleus collisions at $\sqrt{s_{NN}} = 20 \text{ GeV}$ per nucleon pair found that the positrons had a higher average energy than the electrons [10]. However, the atomic electrons in the target could have contributed to the result. Figure 3 compares the p_T spectra of the produced electron and positron; the two spectra are very similar. No asymmetry is seen beyond the experimental uncertainties.

In addition, we have measured the fraction of events with a single neutron in each ZDC to be 0.06 ± 0.04 (3 out of 52). This is consistent with the single neutron fraction observed in similarly tagged ρ photoproduction [13], supporting the notion of independence assumed in the factorization, Eq. (1).

In conclusion, we have observed e^+e^- production accompanied by nuclear excitation in gold-on-gold ion collisions at a center of mass energy of 200 GeV per nucleon pair. The cross section, pair mass, and angular and rapidity distributions are in agreement with two calculations, one using equivalent photons, and the other a lowest-order QED calculation. The pair p_T spectrum agrees with the QED calculation, but not the equivalent photon calculation. Lowest-order QED describes our data. We set a limit on higher-order corrections to the cross section, $-0.5\sigma_{\text{QED}} < \Delta\sigma < 0.2\sigma_{\text{QED}}$ at a 90% confidence level. The electron and positron p_T spectra are similar, with no evidence of higher-order corrections due to interference.

We thank Kai Hencken for providing the results of his QED calculation, and Joakim Nystrand and Anthony Baltz for the nuclear breakup subroutines used in the EPA calculation. We thank the RHIC Operations Group and RCF at BNL, and the NERSC Center at LBNL for their support.

This work was supported in part by the HENP Divisions of the Office of Science of the U.S. DOE; the U.S. NSF; the BMBF of Germany; IN2P3, RA, RPL, and EMN of France; EPSRC of the United Kingdom; FAPESP of Brazil; the Rus-

sian Ministry of Science and Technology; the Ministry of Education and the NNSFC of China; SFOM of the Czech Republic, FOM and UU of the Netherlands, DAE, DST, and CSIR of the Government of India; and the Swiss NSF.

-
- [1] G. Baur *et al.*, Phys. Rep. **364**, 359 (2002); F. Krauss, M. Greiner, and G. Soff, Prog. Part. Nucl. Phys. **39**, 503 (1997).
 - [2] G. Baur and L. G. Ferreira Filho, Phys. Lett. B **254**, 30 (1991).
 - [3] K. Rumrich *et al.*, Phys. Rev. Lett. **66**, 2613 (1991).
 - [4] D. Yu. Ivanov, A. Schiller, and V. G. Serbo, Phys. Lett. B **454**, 155 (1999).
 - [5] H. Davies, H. A. Bethe, and L. C. Maximon, Phys. Rev. **93**, 788 (1954).
 - [6] R. N. Lee, A. I. Milstein, and V. M. Strakhovenko, hep-ph/0310108.
 - [7] A. J. Baltz and L. D. McLerran, Phys. Rev. C **58**, 1679 (1998); A. J. Baltz, Phys. Rev. Lett. **78**, 1231 (1997); A. J. Baltz, Phys. Rev. C **68**, 034906 (2003).
 - [8] L. D. Landau and E. M. Lifshitz, Phys. Z. Sowjetunion **6**, 244 (1934); G. Racah, Nuovo Cimento **14**, 93 (1937).
 - [9] R. N. Lee and A. I. Milstein, Phys. Rev. A **61**, 032103 (2000); A. J. Baltz, Phys. Rev. C **68**, 034906 (2003).
 - [10] C. R. Vane *et al.*, Phys. Rev. A **50**, 2313 (1994).
 - [11] R. Baur *et al.*, Phys. Lett. B **332**, 471 (1994).
 - [12] V. Morozov, Ph.D. dissertation, University of California at Berkeley, 2003, nucl-ex/0403002.
 - [13] STAR Collaboration, C. Adler *et al.*, Phys. Rev. Lett. **89**, 272302 (2002).
 - [14] A. Baltz, S. Klein, and J. Nystrand, Phys. Rev. Lett. **89**, 012301 (2002).
 - [15] K. Hencken, D. Trautmann, and G. Baur, Z. Phys. C **68**, 473 (1995).
 - [16] G. Baur *et al.*, Nucl. Phys. **A729**, 787 (2003).
 - [17] A. J. Baltz, M. J. Rhoades-Brown, and J. Weneser, Phys. Rev. E **54**, 4233 (1996).
 - [18] V. M. Budnev *et al.*, Phys. Rep., Phys. Lett. **15**, 181 (1975).
 - [19] M. Vidovic, M. Greiner, C. Best, and G. Soff, Phys. Rev. C **47**, 2308 (1993).
 - [20] S. Klein and J. Nystrand, Phys. Rev. Lett. **84**, 2330 (2000).
 - [21] S. Klein and J. Nystrand, Phys. Rev. C **60**, 014903 (1999).
 - [22] K. Hencken, G. Baur, and D. Trautmann, Phys. Rev. C **69**, 054902 (2004); A. Alscher *et al.*, Phys. Rev. A **55**, 396 (1997).
 - [23] K. Hencken (private communication).
 - [24] M. Anderson *et al.*, Nucl. Instrum. Methods Phys. Res. A **499**, 659 (2003); M. Anderson *et al.*, *ibid.* **499**, 679 (2003).
 - [25] F. S. Bieser *et al.*, Nucl. Instrum. Methods Phys. Res. A **499**, 766 (2003).
 - [26] C. Adler *et al.*, Nucl. Instrum. Methods Phys. Res. A **470**, 488 (2001).
 - [27] C. Adler *et al.*, Phys. Rev. Lett. **87**, 112303 (2001).
 - [28] S. J. Brodsky and J. R. Gillespie, Phys. Rev. **173**, 1011 (1968).